Observational Study

Medicine®

OPEN

Identification of differential expressed PE exosomal miRNA in lung adenocarcinoma, tuberculosis, and other benign lesions

Yan Wang, BS[a,b], Yan-Mei Xu, BS[a], Ye-Qing Zou, BS[c], Jin Lin, BS[a], Bo Huang, MD[a], Jing Liu, MD[a], Jing Li, BS[d], Jing Zhang, BS[a], Wei-Ming Yang, BS[a], Qing-Hua Min, BS[a], Shu-Qi Li, BS[a], Qiu-Fang Gao, BS[a], Fan Sun, BS[a], Qing-Gen Chen, BS[a], Lei Zhang, BS[a], Yu-Huan Jiang, BS[a], Li-Bin Deng, PhD[a,e,*], Xiao-Zhong Wang, MD[a,*]

Abstract

Pleural effusion (PE) is a common clinical complication of many pulmonary and systemic diseases, including lung cancer and *tuberculosis*. Nevertheless, there is no clinical effective biomarker to identify the cause of PE. We attempted to investigate differential expressed exosomal miRNAs in PEs of lung adenocarcinoma (APE), *tuberculous* (TPE), and other benign lesions (NPE) by using deep sequencing and quantitative polymerase chain reaction (qRT-PCR). As a result, 171 differentiated miRNAs were observed in 3 groups of PEs, and 11 significantly differentiated exosomal miRNAs were validated by qRT-PCR. We identified 9 miRNAs, including miR-205-5p, miR-483-5p, miR-375, miR-200c-3p, miR-429, miR-200b-3p, miR-200a-3p, miR-203a-3p, and miR-141-3p which were preferentially represented in exosomes derived from APE when compared with TPE or NPE, while 3 miRNAs, including miR-148a-3p, miR-451a, and miR-150-5p, were differentially expressed between TPE and NPE. These different miRNAs profiles may hold promise as biomarkers for differential diagnosis of PEs with more validation based on larger cohorts.

Abbreviations: AC = adenocarcinoma, APE = pleural effusion of lung adenocarcinoma, EMT = epithelial–mesenchymal transition, EVs = extracellular vesicles, MET = mesenchymal–epithelial transition, NPA = nanoparticle analysis, NPE = pleural effusion of benign lesions, NSCLC = nonsmall cell lung cancer, PE = pleural effusion, qRT-PCR = quantitative polymerase chain reaction, RISC = RNA-induced silencing complexes, SCC = squamous cell carcinoma, SEM = scanning electron microscopy, TNF = tumor necrosis factor, TPE = pleural effusion of *tuberculous*, VEGF = vascular endothelial growth factor.

Keywords: deep sequencing, exosome, miRNA, pleural effusions

1. Introduction

Pleural effusion (PE) is common but abnormal accumulation of fluid in the pleural space. Lung cancer and *tuberculosis* are the 2 most frequent causes of exudative PEs, suggesting pleural involvement of lesions.[1,2] Nonsmall cell lung cancer (NSCLC) accounts for more than 80% of lung cancer types and these include adenocarcinoma (AC) and squamous cell carcinoma (SCC).[3] Lack of specific clinical presentations and biochemical markers complicate the process of distinguishing of PE etiology.

Using Light's criteria to classify PEs into exudates and transudates is a preliminary step and then other diagnostic methods, such as conventional diagnostic methods, can be used characterize PEs.[2,4–6] Cytology can be used to confirm 30% to 60% malignant PEs in advanced disease stages but constant variation depends on tumor origin confused us. Immunocytochemistry can be used to study pleura, but sensitivity or specificity is not optimal.[7] Histological diagnosis and better imaging can help when combined with thoracoscopy, but this aggressive and invasive approach can cause complications and increase morbidity as well. Soluble mediators were also found to contribute to PEs: vascular endothelial growth factor (VEGF), tumor necrosis factor (TNF), endothelin,[8] Interleukin (IL)-27,[9] and IL-6.[10–12] These markers are more sensitive and specific than conventional diagnostic methods, while its accuracy is limited when PE is of diverse sources and markers may be difficult to measure. In

Editor: Peng Qi.

YW, Y-MX, and Y-QZ are the joint first authors.

This work was supported by the National Natural Science Foundation of China (No. 81271912, No. 81360083), the Youth Innovation Team of the Second Affiliated Hospital of Nanchang University (No. 2016YNTD12002), and Science and Technology Department of Jiangxi Province, China (No. 20143BBM26060).

The authors have no conflicts of interest to disclose.

Supplemental Digital Content is available for this article.

[a] Department of Clinical Laboratory, The Second Affiliated Hospital of Nanchang University, Jiangxi, [b] Department of Hematology, The Affiliated Hospital of Guizhou Medical University, Guizhou, [c] The Key Laboratory of Molecular Medicine, The Second Affiliated Hospital of Nanchang University, [d] Department of Clinical Laboratory, The First Affiliated Hospital of Nanchang University, [e] Institute of Translational Medicine, Nanchang University, Jiangxi, China.

[*] Correspondence: Xiao-Zhong Wang and Li-Bin Deng, Department of Clinical Laboratory, The Second Affiliated Hospital of Nanchang University, No. 1 Min De Road, Nanchang, Jiangxi 330006, China (e-mails: jzteam@163.com; nuc_genome@163.com).

Medicine (2017) 96:44(e8361)

Received: 15 December 2016 / Received in final form: 17 August 2017 / Accepted: 14 September 2017

http://dx.doi.org/10.1097/MD.0000000000008361

addition, the markers are poorly stable as disease indicators, which may cause misdiagnosis due to degradation. Thus, ≈30% of PE is attributed to unknown causes. Recently, circulating exosomes for differential diagnosis has drawn considerable attention.

Exosomes, membrane-bound vesicles of 30 to 100 nm diameter, occur in almost all biological fluids.[13] They are homogeneous in size and can be differentiated from extracellular vesicles (EVs) such as microvesicles and large oncosomes.[14,15] Exosomes can mediate the exchange of intricate intercellular messages with highly heterogeneous signaling factors, including miRNAs, mRNAs, DNA, and proteins.[16] Numerous studies have revealed exosomal donor-cell-specific signatures,[17–19] and its nature and abundance of the molecular cargo are often influenced by donor cell pathological status and origin.[20] Besides, exosomal miRNAs can exist stably in body fluids, and related to information of maternal tissue or cell based on miRNA expression and composition.[21,22] Intriguingly, exosomal miRNAs likely interact with RNA-induced silencing complexes (RISC), mediating miRNA formation and sorting.[23,24] AGO2 knockout was reported to change the types or abundance of preferentially exported miRNA,[25] so circulating exosomal miRNAs may be potential noninvasive diagnostic biomarkers.[26–28]

We previously deep sequenced EVs derived from PEs of NSCLC and tuberculosis, acquired a group of differential expressed miRNAs.[29] However, the results were conflicting due to EVs heterogeneity and generalized histological subtypes.[30,31] Relative to EVs, exosomes are better as the liquid biopsy specimens for their homogeneity in size and contents (Extended Table 1, http://links.lww.com/MD/B922). To identify the potential biomarkers to differentiate NSCLC, AC, and SCC we collected 3 groups of exosomes rather than EVs for deep sequencing and qRT-PCR analysis. Our study would contribute to differentiate diagnosis of these diseases.

2. Materials and methods

2.1. Patients

The study protocol was approved by the Ethics Committee of the Second Affiliated Hospital of Nanchang University, China, and informed consent was obtained from each patient. PE samples were collected before clinical treatment from November 2013 to November 2015 at the Second Affiliated Hospital of Nanchang University. The eligible PE samples were selected according to the following included criteria: exudate based on Light's criteria;[2,32] adenocarcinoma tumor cells in PEs or in pleural biopsy specimens were defined as APE; the presence of acid fast bacilli and *M tuberculosis* in PEs met criteria for TPE; undiagnosed exudates negative for cancer according to histological or cytological criteria were classified as benign controls (NPE). Meanwhile, PE samples were excluded when patients were diagnosed as atelectasis, pulmonary embolism, obstructive pneumonia, or other primary tumor diseases. For each patient, an initial diagnostic thoracenteses was performed when patients sitting upright after local infiltration with lignocaine. PE was obtained via needle aspiration and aspirate volumes were recorded.

2.2. Exosome precipitation

Exosomes were isolated from 120 mL PEs with differential centrifugations as previously described.[29] To remove cells and debris, PE supernatants were sequentially centrifuged for 20 minutes at 1200 × g and 30 minutes at 10,000 × g. To remove particles greater than 200 nm, supernatants were filtered through 0.22 μm pore filters and rinsed with PBS using ultracentrifugation (Optima L-80XP Ultracentrifuge, Beckman Coulter, Beckman) for 1 hours at 120,000 × g twice. All the steps were carried out at 4°C. Finally, the pellets were resuspended in PBS and stored at −80°C for further use.

2.3. Scanning electron microscopy (SEM) and nanoparticle analysis (NPA)

SEM (FEI XL30, The Netherlands) was used to visualize exosome preparations. To begin the SEM analysis, ultracentrifuged pellets were fixed with 3.5% glutaraldehyde overnight at 4°C. After removing glutaraldehyde via centrifugation, fixed exosomes were dehydrated with an ascending sequence of ethanol (15%, 30%, 60%, 80%, and 100%). Afterward, the samples were dried at room temperature for 24 hours on an aluminum sheet, and viewed using SEM with gold-palladium sputtering. Moreover, pellet size was measured by Mastersizer 2000E nanoparticle analysis (NPA) with Beckman Coulter (Indianapolis, IN). After exosome precipitation, the pellets were resuspended in 0.5 mL PBS and sent for NPA. Each experiment was carried out in triplicate.

2.4. Western blot

Total protein was prepared from exosomes pellet by using a Protein Extraction Kit (Applygen, Beijing, China) and separated via 10% SDS-PAGE, then transferred onto 0.22 μm PVDF membranes. After 3 hours blocking with 5% nonfat milk, membranes were incubated with primary rabbit antihuman antibodies (Abcam, London, UK) for Alix and CD63 (1:2000) overnight. Secondary goat antirabbit HRP-linked antibody (cwbiotech, Beijing, China) was applied for 1 hour (1:10,000) in blocking buffer. Finally, immunoreactive bands were visualized with an ECL kit (Thermo-Fisher, Shanghai, China).

2.5. Quantitative RT-PCR (qRT-PCR) preparation

Total RNA was extracted from exosomes pellet with TRIzol reagent (Invitrogen, California). Quantity and quality were assessed through spectrophotometer (260/280 nm) (Thermo-Scientific, Shanghai, China), which selected eligible RNA for deep sequencing analysis or qRT-PCR validation. Subsequently, cDNA was synthesized in the presence of reverse transcription (RT) primer using a SYBR Premix Ex Taq Kit (RiboBio, Guangzhou, China). After the amplification procedure (40 cycles for 10 seconds at 95°C, 30 seconds at 60°C, 1 second at 70°C), miRNA level was quantitatively determined using a real-time RT-PCR kit, in which miR-39-3p was set as an external control in the analysis of each miRNA.

2.6. Small RNA deep sequencing

To characterize miRNA expression profiling, small RNA sequencing and data analysis were conducted by a commercial service (RiboBio, Guangzhou, China). Initially, total RNA samples were sent for RT and PCR amplification. After ligation of 5′ and 3′ adaptors to each end, cDNA were separated on a polyacrylamide gel and low-quality reads were excised to produce clean reads (18–30 nucleotide RNA molecules). Clean reads were aligned to a mature miRNA human genome sequence in miRBase (v21) to identify known miRNAs and used for sequence analysis on an Illumina HiSeq 2500 platform. Differential expression of miRNA among 3 groups was analyzed using a cluster analysis and expressed as the heatmaps (red: overexpressed miRNAs; green: underexpressed miRNAs).

Table 1

The baseline characteristics of eligible patients in 3 groups.

Characteristics	Group A	Group B	Group C
Histology	Lung adenocarcinoma	Pulmonary tuberculosis	Benign
Males/females	4/2	4/3	1/1
Age (mean ± SD, years)	52 ± 4.1	39.2 ± 5.7	47 ± 2.6
Sample no. for analysis*	A1, A2, A3	B1, B2, B3	C1, C2
Clinical sample no.*	3–4, 5–6, 7–8	9–10, 11–12, 13–15	1,2

All the patients were given an initial diagnosis without treatment or complications at the time of sample collection.
* Mixed sample analysis ensured good limits for sequence detection. Samples no. 3 and 4 were mixed for sequencing as sample no. A1.

2.7. Bioinformatic analyses

During Illumina HiSeq 2500 analysis, miRNA expression (reads/million [RPM] clean tags) was normalized with the formula: RPM = (number of reads mapping to miRNA)/(number of reads in clean date) $\times 10^6$. Next, we calculated the fold changes in expression levels via formula of $\log_2^{\text{ratios}}$ (fold change = $\log_2^{(\text{sample group 1/group 2})}$). Significant differences among groups were assessed using edgeR analysis. All the data were expressed as mean ± SD and *P* values below.05 were considered statistically significant.

3. Results

3.1. Patient collection

A total of 168 PE samples with unknown causes were successfully collected. We got 22 eligible samples after the exclusion of transudate or PEs with atelectasis, pulmonary embolism, obstructive pneumonia, or other primary tumor disease. Six APE samples were used and mixed to 3 samples in group A for deep sequencing analysis. In the same way, 3 samples from group B mixed from 7 TPE specimens were selected, and 2 NPE samples were kept for deep sequencing analysis. The characteristics of included patients were established in Table 1 and the study design was shown in Fig. 1.

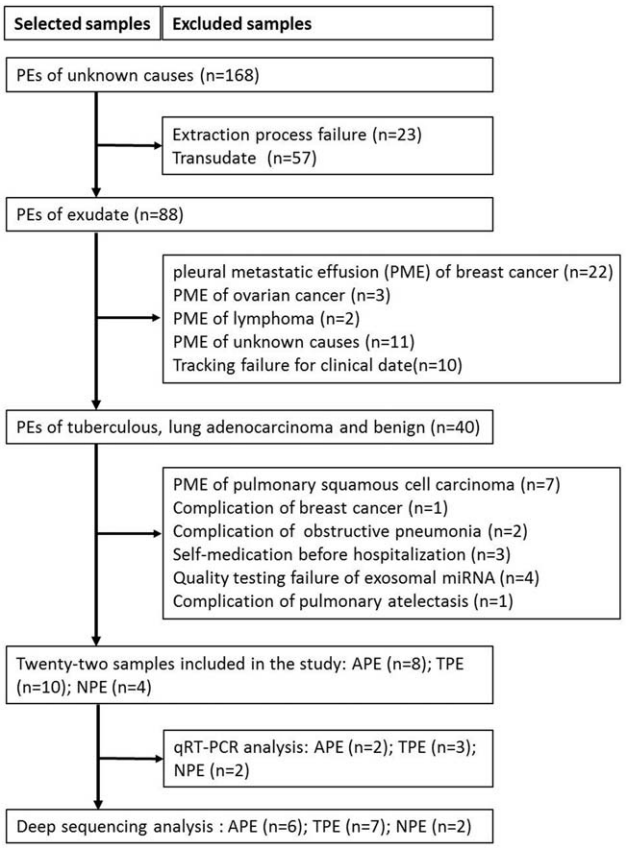

Figure 1. Flow chart of screening eligible samples.

3.2. Characterization of exosomes from PEs

Exosomes were successfully purified through a series of microfiltration and differential centrifugation steps modified by previously description.[29] Results from SEM in Fig. 2 showed round structures with heterogeneous size (30–100 nm), consistent with known vesicular morphology of exosomes.[33] Current criteria to distinguish EVs from exosomes are mainly based on size and density. To do further validation, the particle size distribution of exosomes purified from PEs in NPA results was approximately 30 to 100 nm in diameter (Fig. 3). Pure exosomes were obtained via filtering as described before.[29] Western blot then confirmed the positive typical exosome features of Alix and CD63 (Fig. 4).[34–36]

3.3. Overview of small RNA sequencing data

Deep sequencing analysis of small RNA libraries for 6 APE, 7 TPE, and 2 NPE samples produced raw, clean, and annotated

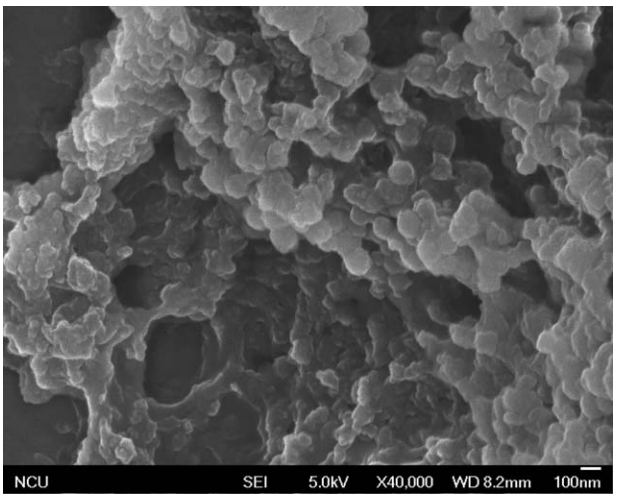

Figure 2. Verification of the exosomal preparation. The morphologic characterization of exosomes purified from PEs was observed by SEM, which showed round structures with heterogeneous size. PE = pleural effusion, SEM = scanning electron microscopy.

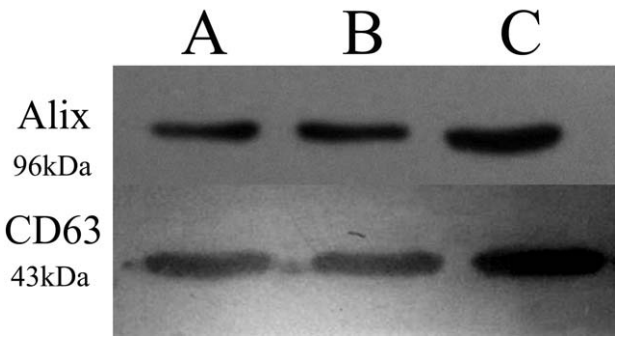

Figure 3. The particle size distribution of exosomes purified from PEs was approximately 30 to 100 nm in diameter. PE = pleural effusion.

clean reads, as well as the corresponding total RNA reads in succession (Extended data Table 2, http://links.lww.com/MD/B922). After miRBase (v21) examination corresponding to each sample, more than 470 miRNAs were detected in clinical samples, indicating different miRNA profiles among samples (Extended data Table 3, http://links.lww.com/MD/B922).

3.4. MicroRNAs profiling and selection of differential microRNAs

MiRNA-enrichment analysis for exosomes purified from APE, TPE, and NPE was conducted and 171 miRNAs were statistically differentially expressed by applying the screening condition at $P < .05$ (Table 2). Further filtering the miRNAs with the condition of less than 3-fold changes and 100 expression counts yielded 23 highly-represented miRNAs, which could distinguish APE from other groups. Taking the repetition of miRNA and expression balance (std. $P < .70$) of samples in 1 group into consideration, 9 of 23 miRNAs were eventually selected for the identification of APE and all 9 miRNAs were represented in the APE library (Table 3). For example, miR-205-5p owned more than 225 RPM in APE, holding 21-fold changes when compared

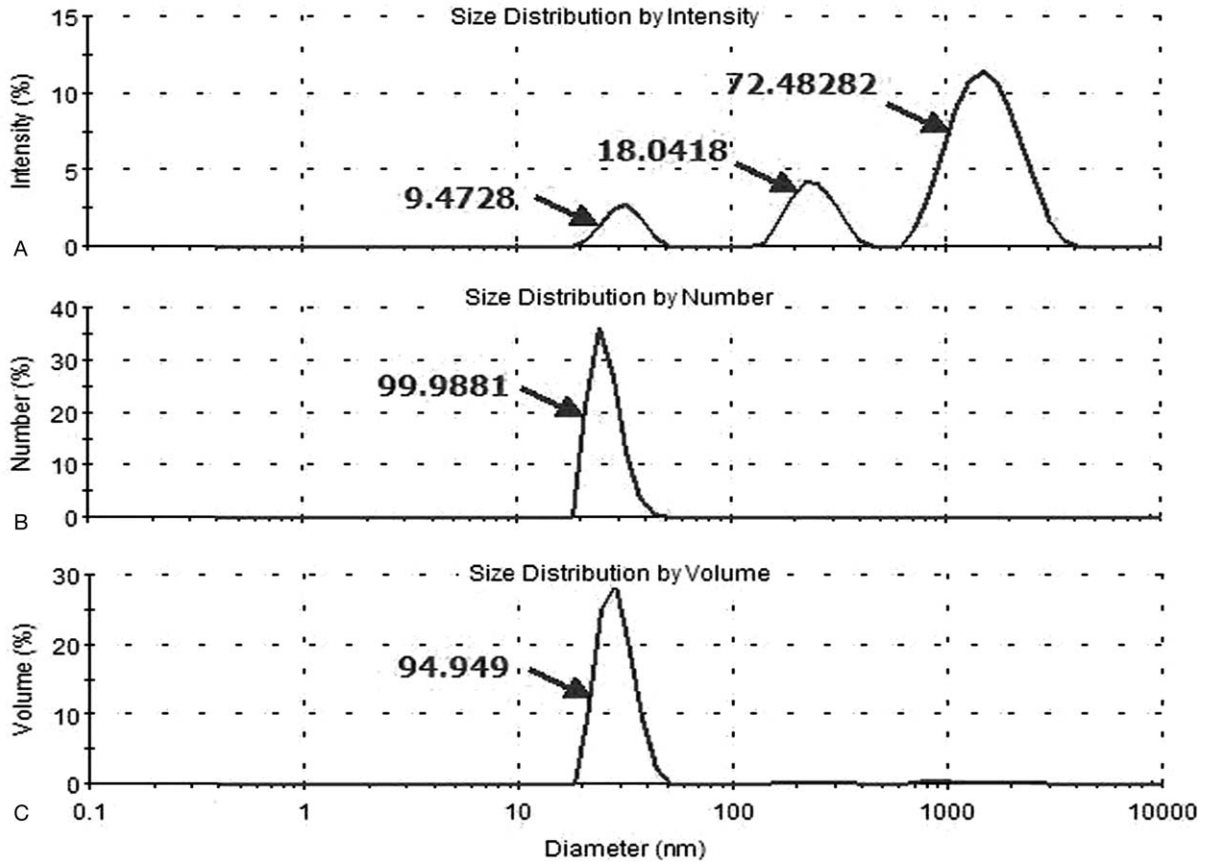

Figure 4. Western blot of 10 to 20 g of proteins extracted from exosomal pellets were positive for exosome-associated proteins (Alix and CD63).

Table 2

Selection criteria of eligible miRNAs.

	A/C		B/C		A/B		
Selection criteria	**Up**	**Down**	**Up**	**Down**	**Up**	**Down**	**Total**
$P < .05$	47	35	12	21	46	10	171
$P < .05$, $\lvert\log_2^{(\text{fold-change})}\rvert > 2$, RPM > 100	14	8	1	4	13	5	45
$P < .05$, $\lvert\log_2^{(\text{fold-change})}\rvert > 3$, RPM > 100	12	—	—	—	11	—	23

—: No eligible genes corresponding to the selection criteria. A: Exosomal miRNAs derived from APE. B: Exosomal miRNAs derived from TPE. C: Exosomal miRNAs derived from NPE.

Table 3

MiRNAs datasets enriched in different exosomes.

miRNA_ID	Group A (APE)	Group B (TPE)	Group C (NPE)	$\lvert log_2^{(A/C)} \rvert$	$\lvert log_2^{(B/C)} \rvert$	$\lvert log_2^{(A/B)} \rvert$	NSCLC association
miR-205-5p	225.2479	4.4815	0.0000	21.1030	15.4517*	5.6513	Yes
miR-483-5p	102.8604	0.5959	0.0000	19.9722	12.5410*	7.4312	Yes
miR-375	625.9924	0.1882	0.8566	9.5132	2.1864*	11.6996	Yes
miR-200c-3p	2058.8070	13.7787	9.1430	7.8149	0.5917*	7.2232	Yes
miR-429	239.9334	4.0959	7.4608	5.0071	−0.8651*	5.8722	Yes
miR-200b-3p	2612.7250	49.1205	94.2341	4.7931	−0.9399*	5.7330	Yes
miR-200a-3p	1411.2340	28.5367	43.1419	5.0317	−0.5962*	5.6279	Yes
miR-203a-3p	365.6550	9.1551	15.7356	4.5383	−0.7813*	5.3197	Yes
miR-141-3p	581.2790	43.3310	17.1403	5.0837	1.3380*	3.7457	Yes
miR-148a-3p	4974.3790	2093.6556	12624.2783	1.3436	−2.5921	1.2484*	No
miR-451a	450.5173	155.9044	798.5400	−0.8257*	−2.3567	1.5309*	No
miR-150-5p	2731.7633	5287.7552	1240.2571	1.1391*	2.0920	−0.9528*	No

APE = pleural effusion of lung adenocarcinoma, NPE = pleural effusion of benign lesions, TPE = pleural effusion of *tuberculous*, NSCLC association = miRNA date from the literature, − =miRNA expression (RPM) in the former group was greater than the latter.

* No statistical significance was calculated in comparison between groups ($P < .05$).

with corresponding values in NPE libraries, 5.6-fold changes when compared with TPE libraries. The same of great difference, miR-200b-3p, was enriched in exosomes isolated from APE (more than 2612 RPM).

MiRNAs from TPE and NPE were nearly homogeneous. Three miRNAs (miR-148a-3p, miR-451a, and miR-150-5p) were screened via the second formula in Table 3 and could distinguish TPE from NPE. Cutoff of 2-fold changes was used in this section, which was still sufficient to meet clinically identification criteria. Last, 12 differentiated miRNAs were selected. Cluster analysis, visualized by heatmaps (Fig. 5) showed segregation of the 3 groups. Each column represents a miRNA and each row a sample. Red represents over-expressed miRNAs; green corresponds to under-expressed miRNAs. Significant differences were observed between APE and other groups, whereas TPE and NPE were almost similar except 3 miRNAs (miR-148a-3p, miR-451a, and miR-150-5p).

3.5. Quantitative RT-PCR validation

Twelve highly expressed miRNAs were selected for qRT-PCR validation (Fig. 6). MiR-39-3p, acted as succeed external control, had the least expression variation in TPE, APE, and NPE: 0.03967, 0.01761, 0.08605 respectively. That is to say, the expression pattern of miRNA among 3 groups can be correctly determined. This figure showed that miR-205-5p was under-expressed in APE but highly expressed in previous deep sequencing analysis of Table 3. MiR-148a-3p was the least expressed according to qRT-PCR but the greatest expressed according to deep sequencing in NPE. This discrepancy may be due to small sample size in the validation phase, which means more samples are needed for validation.

4. Discussion

Although it has been 30 years since the discovery of exosomes, more similar observations have reported that exosomes serve important roles in cellular communication and the exosomal process is abnormal in disease.[37] Since its homogeneity over EVs, more and more researchers give priority to exosomes as the study subject. Numerous studies suggest that donor cells can secrete more exosomes compared with healthy cells,[38–40] and the corresponding exosomal content is distinct. According to this feature, many researchers proposed that exosomal miRNAs indicate the disease process,[41,42] can be applied for differentiating diseases,[43,44] which has been equally confirmed in our study. Careful results analysis showed that quite some miRNAs differ among 3 groups of PEs, especially some miRNAs were remarkably highly expressed in 1 group. For this study, 9 miRNAs (miR-200c-3p, miR-200b-3p, miR-200a-3p, miR-429 and miR-141-3p, miR-205-5p, miR-483-5p, miR-375 and miR-203a-3p) were the most abundant profiles in APE when compared with TPE or NPE, and promises to be used to distinguish APE from the other disease states with more validation. Nevertheless, TPE and NPE had nearly similar and low expression of miRNAs compared with APE and only 3 significantly different miRNAs (miR-148a-3p, miR-451a, and miR-150-5p) hold promise to distinguish TPE from NPE.

Five out of the 9 miRNAs significantly differential expressed in APE compared with others (Table 4). Previous studies recommended that miR-200c-3p, miR-200b-3p, miR-200a-3p, miR-429, and miR-141-3p belonged to the miR-200 family and all 5 members were downregulated in cells undergoing epithelial-mesenchymal transition (EMT). Ectopic expression of miR-200 seconds in mesenchymal cells induced mesenchymal-epithelial transition (MET) and miR-200 family members could regulate EMT by repressing expression of ZEB1/ZEB2 (zinc-finger- and homeobox-containing transcriptional regulator delta-crystallin enhancer-binding factor) and Smad-interacting protein 1.[45–48] Namely, high miR-200 expression inhibits lung adenocarcinoma cell invasion and was associated with shorter overall survival in patients with lung adenocarcinoma.[49,50] However, data from systematic analysis of relevance between miR-200 and EMT were variable, which indicated high miR-200 expression in metastatic cancer. Using a mesenchymal-specific Cre-mediated fluorescent marker switch system in spontaneous breast-to-lung metastasis models, Fischer[51] observed that inhibiting EMT by overexpressing miR-200 did not affect the development of lung metastasis. Recent studies established high miR-200 expression in breast or ovarian cancer and ectopic expression of miR-200 conferred metastatic ability in poorly metastatic tumor cells via extracellular vesicles.[52,53] Consistent with these findings, the miR-200 family is abundant in exosomes derived from APE in our study, suggesting a correlation between miR-200 and PE formation.

The other 4 miRNAs from 9 microRNAs were also previously reported to be related to lung cancer one way or another (Table 5). Data reported here indicated that miR-205-5p was the

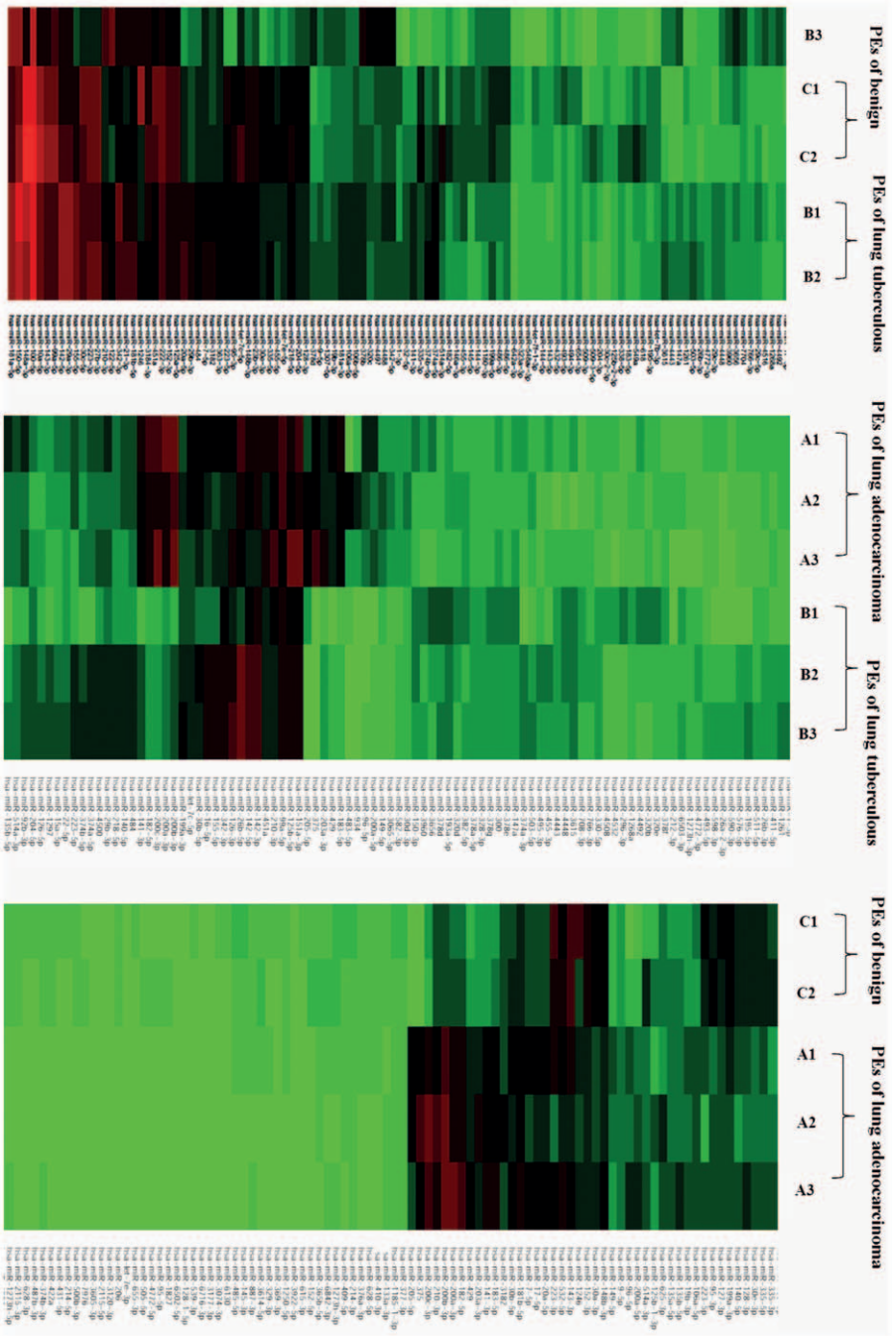

Figure 5. Cluster analysis heatmap of miRNA in 3 kinds of PEs. miRNAs based on global miRNA expression analyses in APE (A1–A3) and NPE (C1–C2). MiRNAs based on global miRNA expression analyses in (A1–A3) APE and (B1–B3) TPE. MiRNAs based on global miRNA expression in (B1–B3) TPE and (C1–C2) NPE samples. Each column represents an miRNA and each row is a sample. Red represents over-expressed miRNAs; green is under-expressed miRNAs. APE = pleural effusion of lung adenocarcinoma, NPE = pleural effusion of benign lesions, TPE = pleural effusion of *tuberculous*,

most expressed and could separate APE from NPE (21-fold change) and separate AE from TPE (5.6-fold change). Yanaihara group come to an agreement with our data, reporting that high miR-205 expression positively correlated with progress of lung cancer and associated with poor survival.[54] Rabinowits' group reported similarity between circulating exosomal miRNA and tumor-derived miRNA patterns in patients of lung adenocarcinomas,[42] suggesting a diagnostic efficiency of circulating exosomal miR-205 with specific genes isolated from tumor tissues. Similarly, the experimental study of Zhang and even a meta-analysis reported high expression of circulating miR-205-5p in NSCLC.[26,55] Consistent with the miRNAs described above, miR-203a-3p was highly expressed in APE samples and previous studies indicated that miR-203a was less expressed in NSCLC tissues compared with adjacent nonmalignant tissues.[56]

Most of the above-mentioned miRNAs have been established in our previous study, they owned the same expression pattern with this project. Otherwise, several miRNAs are emerging as

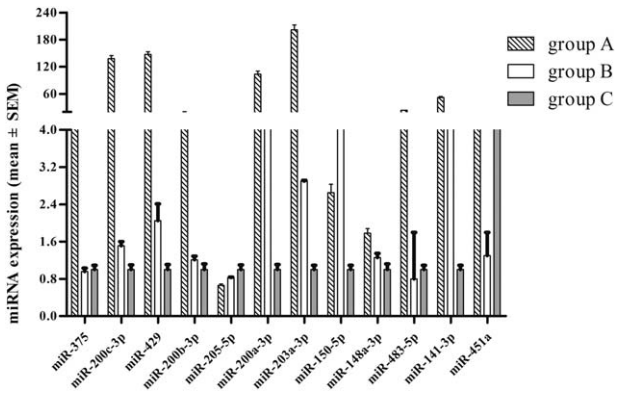

Figure 6. MiRNAs expression overview. MicroRNAs expression from qRT-PCR analysis, with comparative analysis of miRNAs differentially expressed between RT-PCR validation and deep sequencing analysis. RT-PCR = real time polymerase chain reaction, qRT-PCR = quantitative polymerase chain reaction.

different expression level. The differences between 2 studies are assumed to associate with exosomes but EVs, which remains to be proven.

In Wang analysis, miR-483-5p was significantly elevated in NSCLC with more lung adenocarcinoma than squamous cell carcinoma patients, and could be used to distinguish NSCLC from benign nodules (area under the curve 0.979; 95% CI, 0.959–1.0; 86% accuracy).[57] Also previous research suggested miR-483-5p directly targeted 2 putative metastatic suppressors (RhoGDI1 and ALCAM), promoting EMT and increasing invasiveness and metastatic properties of lung adenocarcinoma after activation by the WNT/b-catenin signaling pathway.[58] As far as miR-375, Molina-Pinelo's analysis confirmed that mR-375 was differentially expressed in squamous cell lung cancer compared with adenocarcinoma samples.[59] Claudin-1 is a novel target of miR-375, and high miR-375 expression was correlated with shorter survival time among those with lung adenocarcinoma.[60–62] Moreover, we found miR-9 may be involved in squamous lung cancer by regulating cell cycle-related genes.[63] Benefited from samples limitation of NSCLC to adenocarcinoma, we concluded that miR-483-5p and miR-375 had strong correlation with lung adenocarcinoma, miR-9 has its unique superiority in squamous lung cancer. What is more, miR-148a-3p, miR-451a, and miR-150-5p barely searched in *tuberculous* which prompted new biomarkers in the diagnosis of TPE.

As for the contradictory expression of miR-203a or miR-200 between this study and other literature, we summarized several

Table 4

Brief summary of miR-200 family.

miRNA_ID	Histological subtypes	Specimen	Study type	Expression pattern	Conclusion
miR-200b-3p	AC	Circulating exosomes	Diagnostic studies (cancer versus healthy smokers	Up/down	"Screening test" (miR-378a, miR-379, miR-139-5p, and miR-200b-5p) showed 97.5% sensitivity, 72.0% specificity, AUC ROC of 90.8%. Inhibited lung adenocarcinoma cell invasion and metastasis by targeting Flt1/VEGFR1. Targeting Foxf2 to inhibit invasion and metastasis in lung cancers.
miR-200c miR-141	NSCLC	Carcinoma tissues	Diagnostic studies	Down	High miR-141 and miR-200c expression found to be associated with shorter overall survival in adenocarcinoma patients through MET and angiogenesis (OR, 10.649; P=.002).
miR-429	NSCLC	Carcinoma tissues	Diagnostic studies	Up	ROC curve analysis showed the areas under the ROC curve for serum levels of miR-429 were 0.727.
miR-200a	NSCLC	Cell line	Mechanism research	Up	MicroRNA-200a targeted EGFR and c-Met to inhibit migration and invasion in NSCLC.

AC = adenocarcinoma, AUC = area under the curve, Down = downregulated expression, MET = mesenchymal-epithelial transition, NSCLC = nonsmall cell lung cancer, Up = upregulated expression, VEGF = vascular endothelial growth factor.

Table 5

Brief summary of other differential expressed miRNAs.

miRNA_ID	Histological subtypes	Specimen	Study type	Expression pattern	Conclusion
miR-205-5p	AC	Cell line	Mechanism research	Down	MiR-205 targeted PTEN and PHLPP2 to augment AKT signaling and drive malignant phenotypes
miR-483-5p	AC	Serum	Diagnostic studies (cancer vs benign group)	Down	The panel (miR-483-5p, miR-193a-3p, miR-25, miR-214, and miR-7) was capable of distinguishing NSCLC from benign nodules with an AUC of 0.979 (95% CI, 0.959–1.0) in the US cohort and allowed correct prediction of 86% in the Chinese cohorts.
miR-375 miR-205	NSCLC	Carcinoma tissues	Diagnostic studies	Down	RT-PCR of miR-21, miR-205, and miR-375 identified the AC/SCC histotypes with an accuracy of 96%. MiR-203a downregulation induced ERGIC3 overexpression in NSCLC cells.
miR-203a	NSCLC	Carcinoma tissues	Mechanism research	Up	MiR-203a downregulation induced ERGIC3 overexpression in NSCLC cells.

AC = adenocarcinoma, AUC = area under the curve, Down = downregulated expression, NSCLC = nonsmall cell lung cancer, Up = upregulated expression.

explanations including inconsistent histological subtypes (NSCLC, adenocarcinoma, or squamous cell carcinoma) across different studies,[60,61] various sample types (serum, tissue, cell lines, EVs, or exosomes); diverse controls (healthy smokers,[64] benign nodules,[57] or para-carcinoma tissues[56]), and inconsistent cancer stages (early or advanced during malignant transformation).[65]

In conclusion, exosomal miRNAs expression patterns differ among lung adenocarcinoma, tuberculous, and benign samples. Our results show that a group of 9 miRNAs are preferentially sorted into exosomes derived from APE (miR-205-5p, miR-483-5p, miR-375, miR-200c-3p, miR-429, miR-200b-3p, miR-200a-3p, miR-203a-3p, miR-141-3p), and 3 miRNAs (miR-148a-3p, miR-451a, and miR-150-5p) have differential expression between TPE and NPE. Furthermore, miR-483-5p, miR-375, and miR-429 were validated to be associated with lung adenocarcinoma. These miRNAs may hold promise as biomarkers for diagnosing PEs with verification in larger cohort studies.

References

[1] DePew ZS, Maldonado F. The role of interventional therapy for pleural diseases. Expert Rev Respir Med 2014;8:465–77.

[2] Light RW. Clinical practice. Pleural effusion. N Engl J Med 2002;346: 1971–7.

[3] Villena V, Lopez Encuentra A, Echave-Sustaeta J, et al. [Prospective study of 1,000 consecutive patients with pleural effusion. Etiology of the effusion and characteristics of the patients]. Arch Bronconeumol 2002;38:21–6.

[4] Light RW, Macgregor MI, Luchsinger PC, et al. Pleural effusions: the diagnostic separation of transudates and exudates. Ann Intern Med 1972;77:507–13.

[5] Rodriguez-Panadero F, Romero-Romero B. Current and future options for the diagnosis of malignant pleural effusion. Expert Opin Med Diagn 2013;7:275–87.

[6] Sriram KB, Relan V, Clarke BE, et al. Diagnostic molecular biomarkers for malignant pleural effusions. Future Oncol 2011;7:737–52.

[7] Diacon AH, Van de Wal BW, Wyser C, et al. Diagnostic tools in tuberculous pleurisy: a direct comparative study. Eur Respir J 2003;22:589–91.

[8] Hu Y, Hu MM, Shi GL, et al. Imbalance between vascular endothelial growth factor and endostatin correlates with the prognosis of operable non-small cell lung cancer. Eur J Surg Oncol 2014;40:1136–42.

[9] Yang WB, Liang QL, Ye ZJ, et al. Cell origins and diagnostic accuracy of interleukin 27 in pleural effusions. PLoS One 2012;7:e40450.

[10] Ferreiro L, Toubes ME, Valdes L. [Contribution of pleural fluid analysis to the diagnosis of pleural effusion]. Med Clin (Barc) 2015;145:171–7.

[11] Shu CC, Wang JY, Hsu CL, et al. Diagnostic role of inflammatory and anti-inflammatory cytokines and effector molecules of cytotoxic T lymphocytes in tuberculous pleural effusion. Respirology 2015;20: 147–54.

[12] Na MJ. Diagnostic tools of pleural effusion. Tuberc Respir Dis (Seoul) 2014;76:199–210.

[13] Lin J, Li J, Huang B, et al. Exosomes: novel biomarkers for clinical diagnosis. ScientificWorldJournal 2015;2015:657086.

[14] Gyorgy B, Szabo TG, Pasztoi M, et al. Membrane vesicles, current state-of-the-art: emerging role of extracellular vesicles. Cell Mol Life Sci 2011;68:2667–88.

[15] Shapiro IM, Landis WJ, Risbud MV. Matrix vesicles: are they anchored exosomes? Bone 2015;79:29–36.

[16] Miller IV, Grunewald TG. Tumour-derived exosomes: tiny envelopes for big stories. Biol Cell 2015;107:287–305.

[17] Muturi HT, Dreesen JD, Nilewski E, et al. Tumor and endothelial cell-derived microvesicles carry distinct CEACAMs and influence T-cell behavior. PLoS One 2013;8:e74654.

[18] D'Souza-Schorey C, Di Vizio D. Biology and proteomics of extracellular vesicles: harnessing their clinical potential. Expert Rev Proteomics 2014;11:251–3.

[19] Choi DS, Kim DK, Kim YK, et al. Proteomics of extracellular vesicles: exosomes and ectosomes. Mass Spectrom Rev 2015;34:474–90.

[20] He Y, Lin J, Kong D, et al. Current state of circulating micrornas as cancer biomarkers. Clin Chem 2015;61:1138–55.

[21] Mathivanan S, Ji H, Simpson RJ. Exosomes: extracellular organelles important in intercellular communication. J Proteomics 2010;73: 1907–20.

[22] Gross JC, Chaudhary V, Bartscherer K, et al. Active Wnt proteins are secreted on exosomes. Nat Cell Biol 2012;14:1036–45.

[23] Frank F, Sonenberg N, Nagar B. Structural basis for 5'-nucleotide base-specific recognition of guide RNA by human AGO2. Nature 2010;465: 818–22.

[24] Melo SA, Sugimoto H, O'Connell JT, et al. Cancer exosomes perform cell-independent microRNA biogenesis and promote tumorigenesis. Cancer Cell 2014;26:707–21.

[25] Guduric-Fuchs J, O'Connor A, Camp B, et al. Selective extracellular vesicle-mediated export of an overlapping set of microRNAs from multiple cell types. BMC Genomics 2012;13:357.

[26] Taylor DD, Gercel-Taylor C. MicroRNA signatures of tumor-derived exosomes as diagnostic biomarkers of ovarian cancer. Gynecol Oncol 2008;110:13–21.

[27] Vilming Elgaaen B, Olstad OK, Haug KB, et al. Global miRNA expression analysis of serous and clear cell ovarian carcinomas identifies differentially expressed miRNAs including miR-200c-3p as a prognostic marker. BMC Cancer 2014;14:80.

[28] Silva J, Garcia V, Zaballos A, et al. Vesicle-related microRNAs in plasma of nonsmall cell lung cancer patients and correlation with survival. Eur Respir J 2011;37:617–23.

[29] Lin J, Wang Y, Zou YQ, et al. Differential miRNA expression in pleural effusions derived from extracellular vesicles of patients with lung cancer, pulmonary tuberculosis, or pneumonia. Tumour Biol 2016;[Epub ahead of print].

[30] Tetta C, Ghigo E, Silengo L, et al. Extracellular vesicles as an emerging mechanism of cell-to-cell communication. Endocrine 2013;44:11–9.

[31] Minciacchi VR, Freeman MR, Di Vizio D. Extracellular vesicles in cancer: exosomes, microvesicles and the emerging role of large oncosomes. Semin Cell Dev Biol 2015;40:41–51.

[32] Pastre J, Roussel S, Israel Biet D, et al. [Pleural effusion: diagnosis and management]. Rev Med Interne 2015;36:248–55.

[33] Andre F, Schartz NE, Movassagh M, et al. Malignant effusions and immunogenic tumour-derived exosomes. Lancet 2002;360:295–305.

[34] Thery C, Boussac M, Veron P, et al. Proteomic analysis of dendritic cell-derived exosomes: a secreted subcellular compartment distinct from apoptotic vesicles. J Immunol 2001;166:7309–18.

[35] Bard MP, Hegmans JP, Hemmes A, et al. Proteomic analysis of exosomes isolated from human malignant pleural effusions. Am J Respir Cell Mol Biol 2004;31:114–21.

[36] Colombo M, Moita C, van Niel G, et al. Analysis of ESCRT functions in exosome biogenesis, composition and secretion highlights the heterogeneity of extracellular vesicles. J Cell Sci 2013;126(pt 24):5553–65.

[37] Milane L, Singh A, Mattheolabakis G, et al. Exosome mediated communication within the tumor microenvironment. J Control Release 2015;219:278–94.

[38] Riches A, Campbell E, Borger E, et al. Regulation of exosome release from mammary epithelial and breast cancer cells—a new regulatory pathway. Eur J Cancer 2014;50:1025–34.

[39] Le MT, Hamar P, Guo C, et al. miR-200-containing extracellular vesicles promote breast cancer cell metastasis. J Clin Invest 2014;124:5109–28.

[40] Rodriguez M, Silva J, Lopez-Alfonso A, et al. Different exosome cargo from plasma/bronchoalveolar lavage in non-small-cell lung cancer. Genes Chromosomes Cancer 2014;53:713–24.

[41] Skog J, Wurdinger T, van Rijn S, et al. Glioblastoma microvesicles transport RNA and proteins that promote tumour growth and provide diagnostic biomarkers. Nat Cell Biol 2008;10:1470–6.

[42] Rabinowits G, Gercel-Taylor C, Day JM, et al. Exosomal microRNA: a diagnostic marker for lung cancer. Clin Lung Cancer 2009;10:42–6.

[43] Madhavan B, Yue S, Galli U, et al. Combined evaluation of a panel of protein and miRNA serum-exosome biomarkers for pancreatic cancer diagnosis increases sensitivity and specificity. Int J Cancer 2015;136: 2616–27.

[44] Goldie BJ, Dun MD, Lin M, et al. Activity-associated miRNA are packaged in Map1b-enriched exosomes released from depolarized neurons. Nucleic Acids Res 2014;42:9195–208.

[45] Feng X, Wang Z, Fillmore R, et al. MiR-200, a new star miRNA in human cancer. Cancer Lett 2014;344:166–73.

[46] Gregory PA, Bert AG, Paterson EL, et al. The miR-200 family and miR-205 regulate epithelial to mesenchymal transition by targeting ZEB1 and SIP1. Nat Cell Biol 2008;10:593–601.

[47] Mutlu M, Raza U, Saatci O, et al. Sahin O. miR-200c: a versatile watchdog in cancer progression, EMT, and drug resistance. J Mol Med (Berl) 2016;94:629–44.

[48] Park SM, Gaur AB, Lengyel E, et al. The miR-200 family determines the epithelial phenotype of cancer cells by targeting the E-cadherin repressors ZEB1 and ZEB2. Genes Dev 2008;22:894–907.
[49] Tejero R, Navarro A, Campayo M, et al. miR-141 and miR-200c as markers of overall survival in early stage non-small cell lung cancer adenocarcinoma. PLoS One 2014;9:e101899.
[50] Roybal JD, Zang Y, Ahn YH, et al. miR-200 Inhibits lung adenocarcinoma cell invasion and metastasis by targeting Flt1/VEGFR1. Mol Cancer Res 2011;9:25–35.
[51] Fischer KR, Durrans A, Lee S, et al. Epithelial-to-mesenchymal transition is not required for lung metastasis but contributes to chemoresistance. Nature 2015;527:472–6.
[52] Dykxhoorn DM, Wu Y, Xie H, et al. miR-200 enhances mouse breast cancer cell colonization to form distant metastases. PLoS One 2009;4: e7181.
[53] Muralidhar GG, Barbolina MV. The miR-200 family: versatile players in epithelial ovarian cancer. Int J Mol Sci 2015;16:16833–47.
[54] Yanaihara N, Caplen N, Bowman E, et al. Unique microRNA molecular profiles in lung cancer diagnosis and prognosis. Cancer Cell 2006;9: 189–98.
[55] Luan J, Wang J, Su Q, et al. Meta-analysis of the differentially expressed microRNA profiles in nasopharyngeal carcinoma. Oncotarget 2016;7: 10513–21.
[56] Lin QH, Zhang KD, Duan HX, et al. ERGIC3, which is regulated by miR-203a, is a potential biomarker for non-small cell lung cancer. Cancer Sci 2015;106:1463–73.
[57] Wang C, Ding M, Xia M, et al. A Five-miRNA panel identified from a multicentric case-control study serves as a novel diagnostic tool for ethnically diverse non-small-cell lung cancer patients. EBioMedicine 2015;2:1377–85.
[58] Song Q, Xu Y, Yang C, et al. miR-483-5p promotes invasion and metastasis of lung adenocarcinoma by targeting RhoGDI1 and ALCAM. Cancer Res 2014;74:3031–42.
[59] Molina-Pinelo S, Gutierrez G, Pastor MD, et al. MicroRNA-dependent regulation of transcription in non-small cell lung cancer. PLoS One 2014;9:e90524.
[60] Yoda S, Soejima K, Hamamoto J, et al. Claudin-1 is a novel target of miR-375 in non-small-cell lung cancer. Lung Cancer 2014;85:366–72.
[61] Hamamoto J, Soejima K, Yoda S, et al. Identification of microRNAs differentially expressed between lung squamous cell carcinoma and lung adenocarcinoma. Mol Med Rep 2013;8:456–62.
[62] Patnaik S, Mallick R, Kannisto E, et al. MiR-205 and MiR-375 microRNA assays to distinguish squamous cell carcinoma from adenocarcinoma in lung cancer biopsies. J Thorac Oncol 2015;10:446–53.
[63] Su YH, Zhou Z, Yang KP, et al. MIR-142-5p and miR-9 may be involved in squamous lung cancer by regulating cell cycle related genes. Eur Rev Med Pharmacol Sci 2013;17:3213–20.
[64] Cazzoli R, Buttitta F, Di Nicola M, et al. microRNAs derived from circulating exosomes as noninvasive biomarkers for screening and diagnosing lung cancer. J Thorac Oncol 2013;8:1156–62.
[65] Peter ME. Let-7 and miR-200 microRNAs: guardians against pluripotency and cancer progression. Cell Cycle 2009;8:843–52.